POAC'17
Busan, KOREA

Proceedings of the 24th International Conference on
Port and Ocean Engineering under Arctic Conditions
June 11-16, 2017, Busan, Korea

Comparison of Satellite Imagery Based Ice Drift with Wind Model for the Caspian Sea

Yevgeniy Kadranov[1], Sigitov Anton[1], Sergey Vernyayev[1]

[1] LLP Iceman.kz, Shimkent, Kazakhstan

ABSTRACT

Many factors influencing the movement of ice such as wind, ice concentration, ice thickness, roughness, water currents, Coriolis force, bathymetry, artificial and natural obstacles in the area. Current speeds in the Caspian Sea are relatively small and so the main driving force for ice movements is wind. Therefore, main goal of this work was to study wind-ice movement velocities dependence in the region and check how ice concentration and thickness influence on the movement of ice.

A high number of measurements and observations was made to describe ice drift in the region, although the data was collected areas and usually not publicly available. In our work, we have used timely consequent optical and SAR satellite images to observe ice movements and its displacement over the area. Wind data for the same period and area was taken from wind models. Ice charts were prepared using visual interpretation of satellite imagery. Ice information (concentration, stage of development, floe size) were stored as vector data in SIGRID3 format. The described data has been correlated and analyzed.

The analysis provided in the work can be used for the forecast of short term ice drift on the operational basis and can be the first step for creation of ice drift forecast model for the region of North Caspian Sea. The used data, methods and results of the study are described in this paper.

KEY WORDS: Ice Charting, Ice behavior modeling, Ice drift, Caspian Sea, Optical and SAR Imagery interpretation, Weather model, GFS

INTRODUCTION

The area of North Caspian Sea is of great interest for Oil & Gas industry with the ongoing and projected offshore development of relatively complex oil fields. Ice detection and forecasting is needed for support of winter operations at site and along transit routes of marine supply lines. One of the major concerns is forecasting ice conditions in the region to plan logistics and avoid hazardous or time-consuming ice and weather impact on operations as discussed by Verlaan et al, 2011. As one of the major drivers of ice related hazards to the offshore installations and navigation is drift, it is useful to understand what the factors control the ice drift over the region. Developing the relationship between the forecast weather parameters, local conditions across region and the resulting drift is the way to build a model to predict ice drift in the region. Objective of this project is to study wind induced ice drift in the region and define to what extent ice concentration influence on the resulting displacements based on observations of the relatively mild ice season 2015-2016.

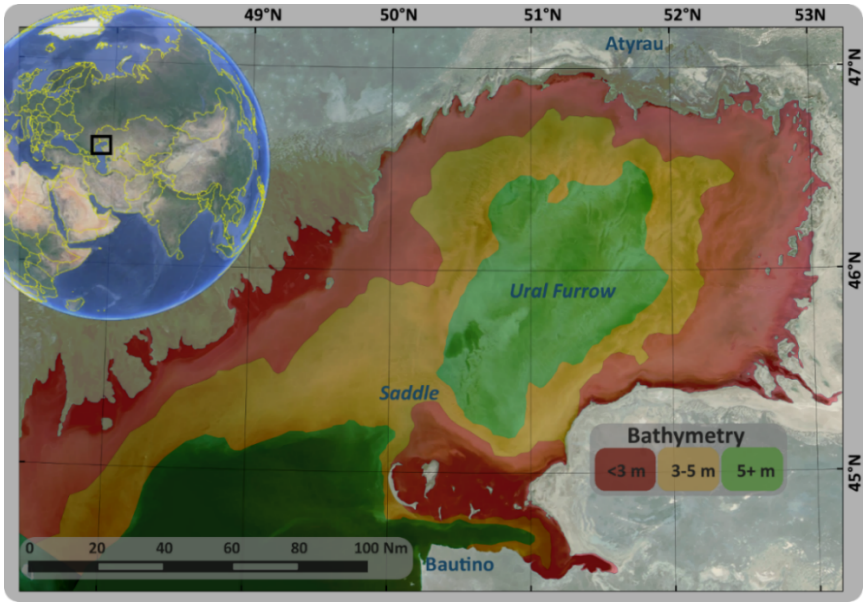

Figure 1. North-East Caspian Sea

North East Caspian Ice Conditions Summary

The North-East Caspian Sea normally stays ice covered from late November-Early December to Late March-Early April. Thermally grown ice thickness typically reaches 40-50 cm along the northern shoreline during an average winter. Ice drift is mostly wind driven and usually occurs over deeper parts of the NE Caspian in the central basin or south of the Saddle area (Figure 1), while ice sheet in the shallower area remains stationary during the major part of the winter. Ice compaction caused by strong wind events often lead to forming of ice features such as stamukhi (grounded rubble mounds) and pressure ridges as well as extensive rafted areas as observed by Crocker et al, 2011. Figure 2 illustrates seasonal variation of ice cover distribution over the last nine seasons 2007-2016.

Based on the analysis of remote sensing data it was noted that the warmer the winter is, more mobile areas are observed over the NE Caspian. Therefore, it was decided that the season 2015-2016 should be used for the comparison of ice drift/wind dependency. As the ice season lasted

from late December to early March, it was shorter than usual. Only 221 FDD (as observed in Atyrau) were collected during this winter – nearly 3 times less than during the average Caspian ice season. Thickest level ice that has grown this season was about 25 cm as calculated by formula derived for this region by Jordaan et al, 2011. Ice conditions during the season 2015-2016 were more dynamic than usual as observed during execution of this project. This was mainly due to milder weather throughout the year (Figure 2). Most Ice in the NE Caspian never consolidated and remained mobile expect for the areas along the shore in the North and East. This created ideal conditions for ice drift analysis based on comparison of satellite images as same ice floe could be tracked for several weeks (while during other seasons, after several days of tracking floe would be deformed with compaction against stationary features or consolidates as part of stationary ice sheet).

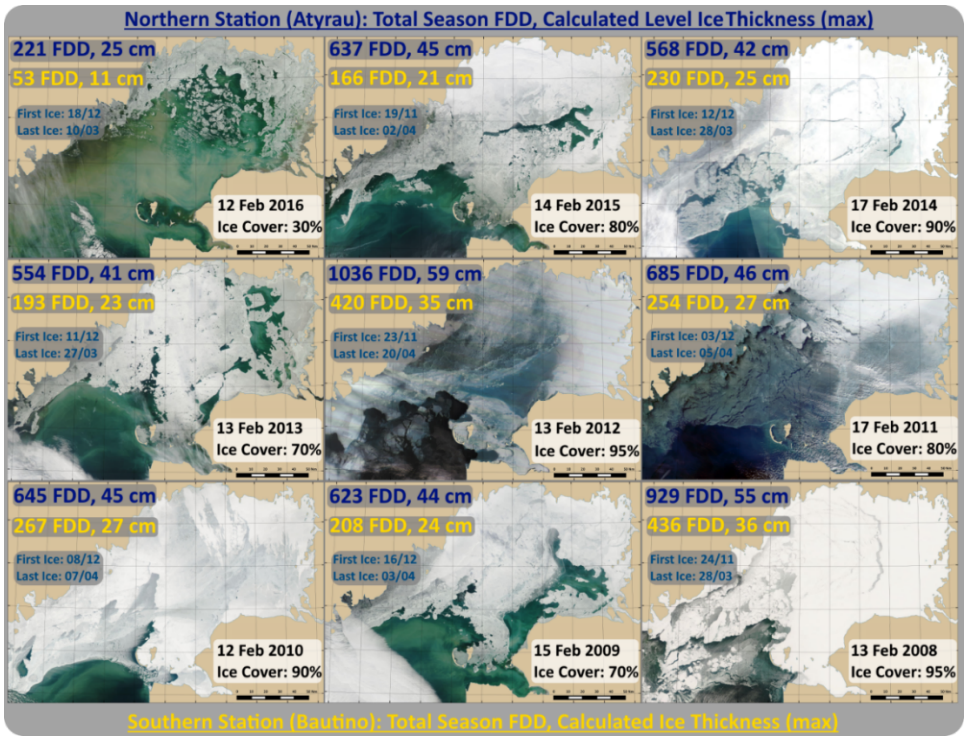

Figure 2. This picture compares 9 ice seasons (from 2007-2008 to 2015-2016). FDD data from NOAA National Centers for Environmental Information.

DATA SOURCES

Satellite Imagery

The major source of data for ice drift measurement within the scope of this project wass satellite images. Choosing between SAR and optical images, SAR is more reliable as it does not depend on cloud cover. However, due to geographical location of the area of interest SAR satellites have revisit time of 3-4 days per week and need to be supplemented with any available optical images.

The season had a fair amount of cloudless days (63% of MODIS images were either clear or partly cloudy as illustrated on Figure 3), which allowed to use optical MODIS Terra and Aqua data from NASA worldview portal intensively.

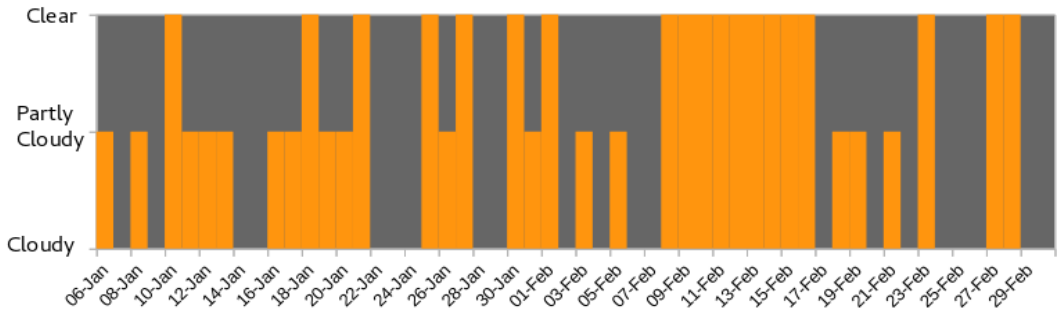

Figure 3. Cloudiness stats for Jan-Mar 2016

Publicly available Sentinel-1 and commercial RISAT-1, TerraSAR-X and Radarsat-2 SAR images were used to close some of the big gaps caused by cloudy sky conditions. Public SAR imagery were taken from Copernicus Science hub, while commercial SAR images were provided by Kongsberg Satellite Services (KSAT).

Ice Drift Data

Ice drift data over the period from 6 January 2015 to 2 March 2016 was gathered by identifying similar ice floes on subsequent images of the series and tracking their displacement. The start date of tracking is the day, when ice cover has established over the major part of the Central Basin of the NE Caspian and South of Saddle.

There were two automated steps of processing satellite images targeted to increase accuracy of the resulting displacement values. Both steps were performed within QGIS environment scripting specific plugins. During the first one, distinctive ice floes were identified on a pair of images and were polygonised as a geo-spatial feature with the following attributes assigned to each feature:

- Start and End Image date
- Floe ID
- Start and End ice concentration around the floe
- Area and perimeter values
- General Comments (rotation of floe, unique behavior, deviation from flow direction)

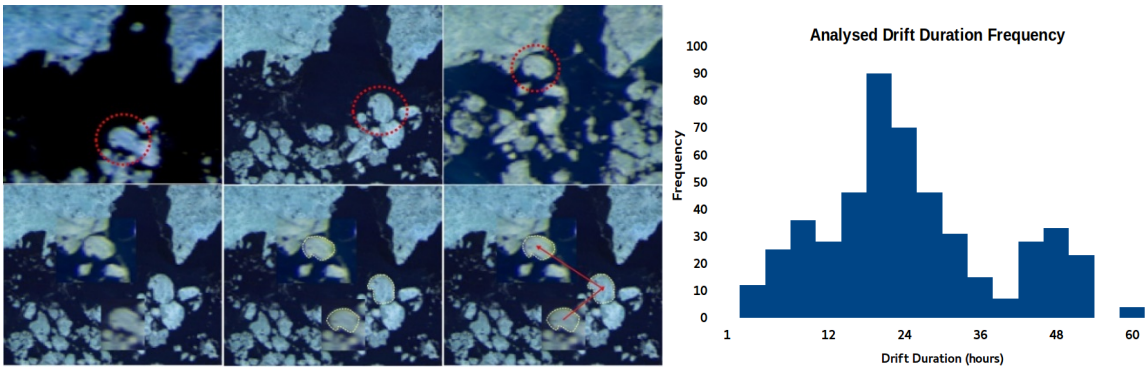

Figure 4. Example of digitizing same ice floe for 3 days (Left). Frequency distribution of drift observations intervals (Right)

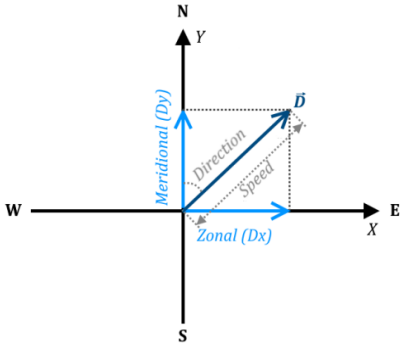

Figure 5. Drift vector and its components

As the second step the other QGIS plugin built vectors between centroids of floes using date and floe id attributes, and calculated vector displacement and direction between adjacent by date floes. Figure 4 (Left) illustrates the example of floes identification and resulting displacement vectors represented in graphical form.

In total for the whole season, 494 ice drift vectors were created and 63 pairs of satellite images were analyzed, making an average of about 8 drift vectors per analysis. The most frequent time interval between two images was about 24 hours, with minimum interval of around 2 hours (between MODIS Terra and Aqua from the same day) and rare maximum of 60 hours (Figure 4 Right).

Drift speed vectors consisting of vector magnitude, direction and two projections on x and y axes were derived from the displacement data. The magnitude of the average ice drift speed vector of the floe was found as an ice floe displacement distance divided by the time interval between the images. Direction of ice drift vector was measured as azimuth between displacement vector measured from true North. The zonal and meridional components of ice drift speed vector were found as orthogonal projections of ice drift speed vector on X (East-West) and Y (North-South) axes correspondingly (**Error! Reference source not found.**). The resulting values were stored in the database.

Ice Conditions Data

Ice conditions description such as total concentrations, partial concentrations, floe sizes and stages of development was prepared and stored as a geo-spatial database in standard SIGRID-3 format for the whole region. Ice conditions data has then been assigned to intersecting ice drift floes with the same date. The resulting ice concentrations were then joined with ice drift vector for each individual vector as attribute containing categories describing it at the start and the end of each track (Table 1). As the season was extremely mild the stage of development more than grey-white ice has never been grown. This has also allowed us to assume the ice thickness conditions were more or less uniform across the sea and neglect its effect on drift behavior.

Table 1. Ice drift concentration categories.

		Final		
		Low (1-3)	**Medium (4-6)**	**High (7-10)**
Initial	**Low (1-3)**	LL	LM	LH
	Medium (4-6)	ML	MM	MH
	High (7-10)	HL	HM	HH

Wind Data

GFS wind analysis model data (10m above Sea Level with spatial resolution of 30x20 nautical miles for the Caspian Sea) was taken as grib file from NOAA datahub, and converted into vector geo-spatial format. The database of wind speed vector components (meridional and zonal) for the season was derived based on four model runs per day, and contained two (+0 hrs and +3 hrs) output array data points from each model run. Considering the data points for resulting database were taken near the model run it was assumed that the dataset was close to real.

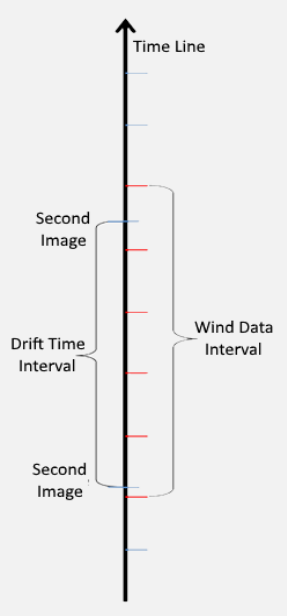

Figure 6. Selected wind data time interval for averaging for each drift interval.

FINAL DATABASE

The data described above was merged into a single database with each record containing corresponding information about ice drift data, wind data and surrounding ice conditions data to perform further analysis. To do that each drift vector's centroid was associated with the nearest GFS grid point. All the wind vectors at that point were averaged within time interval between two satellite images including one more wind vector before and after such interval. The following attributes were derived for each averaged wind vector:

- Averaged zonal (W-E) and meridian(N-S) components of wind vector

- Averaged wind speed (vector magnitude) and direction
- Maximum wind direction deviation from the averaged wind vector using Yamartino method (Yamartino, 1984).

Figure 7 shows wind data as per oceanographic convention (direction toward which the wind is blowing) for the period of observed drift intervals. Presentation of wind vectors with direction 'toward' as opposed to 'from' simplifies the calculus. The drift and wind values of compiled database are in form of drift speed distributions by direction. Most of the wind events have happened towards NW-W and S-SE directions as typical for the region as concluded from years of observations by Nilsen et al, 2011.

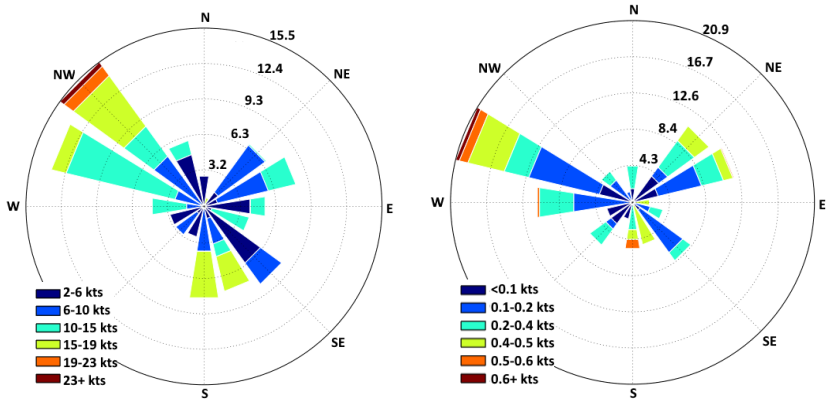

Figure 7. Wind speed and direction (toward) distribution for observed drift intervals (Left) and Ice drift speed and direction distribution (Right).

Flowchart illustrating all the steps of merging the data is schematically shown on Figure 8.

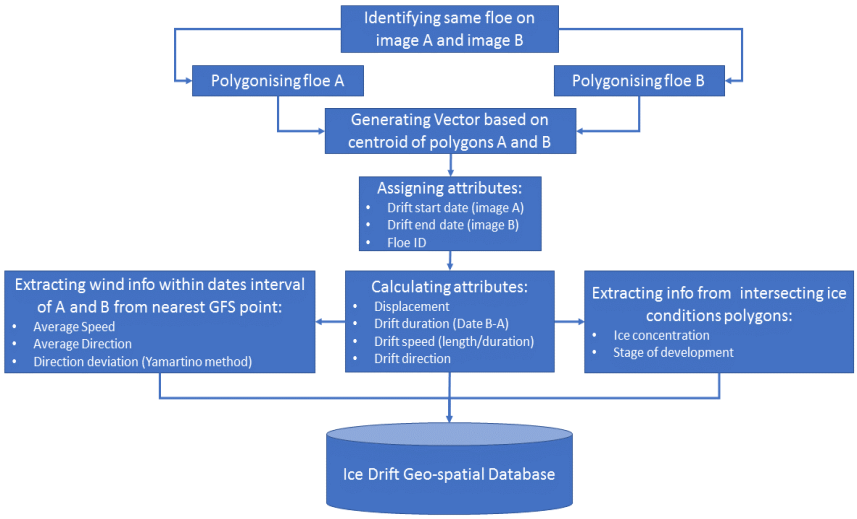

Figure 8. Data flow for Ice Drift geodatabase compilation

Resulting database revealed that ice drift vectors not always correspond to averaged wind vectors. Depending on time interval between the images ice floe could experience variable

range of wind speeds with variable wind directions. For example, wind with even the constant speed can reverse its direction during the time interval, so the real track length of the floe will be much longer than the net floe displacement resulting in significant decrease of average drift speed. Figure 9 shows the wind and drift direction difference versus wind speed illustrating the point above. Most of the used data for wind speeds above 5 knots are within narrow interval of drift-wind difference values as it should be for wind driven drift as we expect in the Caspian.

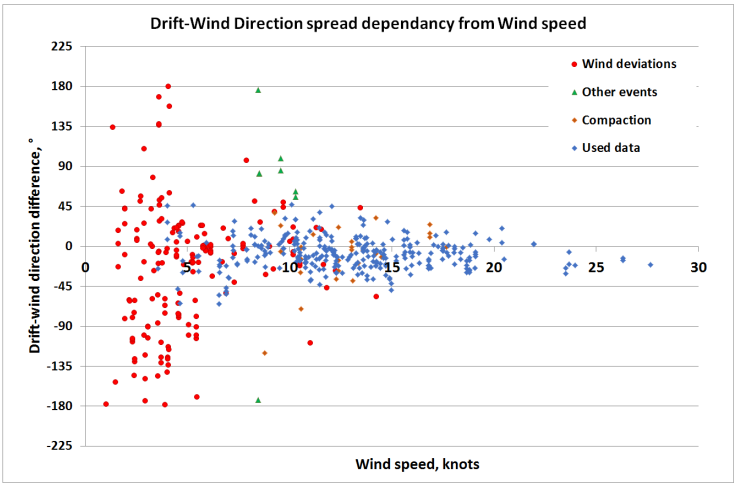

Figure 9. Scatter plot of Drift-Wind directions difference from wind speed

To clean the dataset from the discrepancies caused by the uncertainties of scarce data observations the whole database was filtered to exclude:

1. All drift vectors with the duration of less than 4 hours. It was found that even during homogeneous wind event, accuracy of drift vector length calculation can be significantly affected with image's resolution (250m for MODIS);
2. All the average wind vectors where wind direction deviation was more 60 degrees;
3. Most of the records where average wind speed was lower than 5 knots. As observed during the data compilation, such low values are normally associated with erroneous speed averaging process mentioned above. Low winds events resulting in small displacements with significant difference between drift and wind directions are also regulated by other factors such as currents, ice compaction, sea surface tilt during surge events that become noticeable, but could be neglected with higher winds;
4. Events when the compaction against coastlines or grounded ice features or diverging processes caused by non-homogeneous wind were observed. In this case the frictional forces and internal stresses between ice floes starts to play dominating role in floe behavior
5. Odd cases without reasonable explanation of drift behavior. Sometimes ice floe displacement was observed with incomparable wind speeds. It potentially could be caused by discrepancies in wind model output due to time lag or difficult synoptic situation that could not be handled within model.

As the dataset was cleaned of the cases listed above filtered data has shown clear relationship between wind and drift directions as can be seen on scatter (Figure 10 Right) as one would expect it to be in the region with prevailing wind driven drift as observed by Nilsen et al, 2011. The regression line for wind versus drift speed relationship (Figure 10 Left) showed a relatively

big spread of data around the curve indicating that direct calculation of the drift speed based on one drift/wind ratio is not sufficient for modelling the ice drift in the region.

The distribution of the drift-wind speed ratios frequency shows that the range bin from 2 to 3% is dominant - 41% (Figure 11 Left) and the coefficients in range 1-4% appear for almost 90% of time. This has led us to conclusion we need to segregate these ratios based on concentrations and drift directions as these seemed to be the major factors affecting the coefficient. It can be seen from the Figure 11(Right) that, in general, the ratio coefficient tends to increase with lowering concentration.

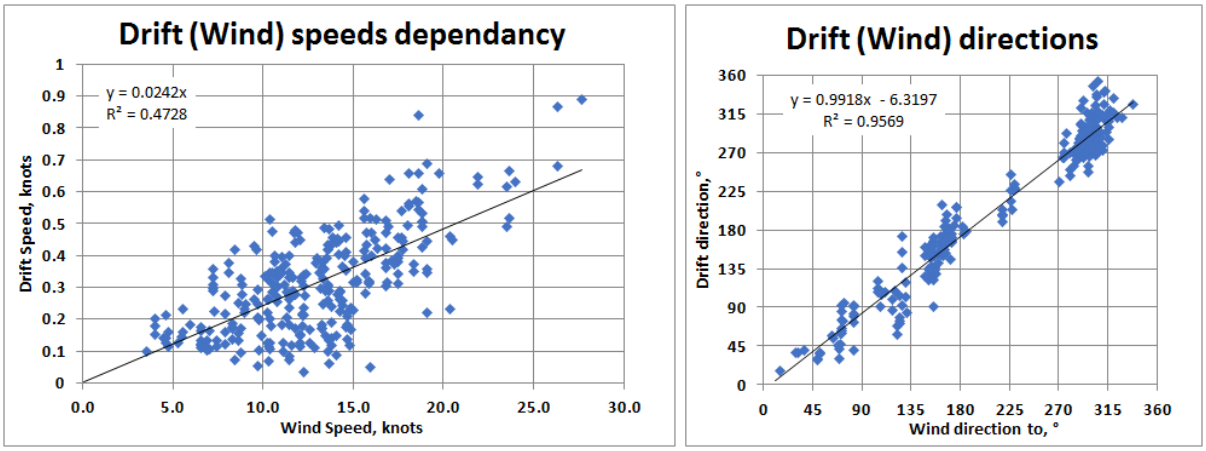

Figure 10. Scatter plot of data for Drift-wind speed (Left) and Drift-wind direction (Right)

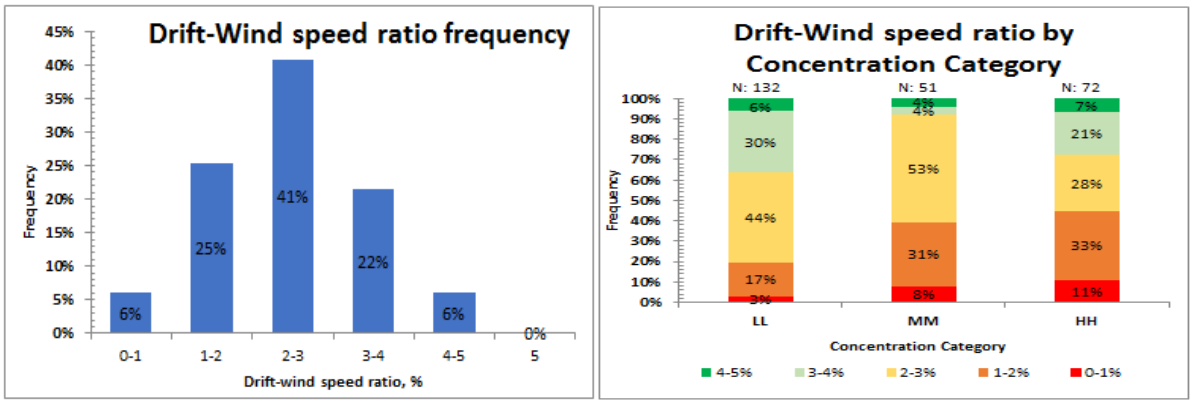

Figure 11. Drift-wind speed ratio frequency distribution (Left). Drift-wind speed ratio frequency by concentration category (Right).

DRIFT MODEL

General ice drift behavior in regards of its dependency to direction and concentrations became clear. Further on, equation (1) presented by Leppäranta (2005) and later simplified by Segboer and Verlaan (2007) was used to describe relationship between drift and wind. As currents measurements results are not publicly available they were accounted within this equation as residual variables described below.

$$\vec{D} = \mathbf{A}\vec{W} + \vec{E},$$

$$\begin{pmatrix} D_x \\ D_y \end{pmatrix} = \begin{pmatrix} a_{11} & a_{12} \\ a_{21} & a_{22} \end{pmatrix} \begin{pmatrix} W_x \\ W_y \end{pmatrix} + \begin{pmatrix} E_x \\ E_y \end{pmatrix} \quad (1)$$

where D_x, D_y are orthogonal zonal (West-East) and meridional (North-South) components of ice drift speed vector $\vec{D}$; W_x, W_y – components of synchronized wind speed vector $\vec{W}$, E_x, E_y – components of residual drift speed vector variation $\vec{E}$ that can't be explained by influence of the wind using linear transformations with matrix **A** with components a_{11}, a_{12}, a_{21}, a_{22}.

A linear regression analysis has been used to determine matrix coefficients a_{11}, a_{12}, a_{21}, a_{22} and E vector components from Eq. (1) based on records of drift vectors and corresponding averaged wind data. The results of the regression analysis are presented in Table 2 and Figure 12.

Table 2. Regression analysis outcome for different drift-wind records set

	All data	Filtered data			
		All	LL	MM	HH
Number of records	493	292	132	51	72
a_{11}	0.0254	0.0257	0.0286	0.0265	0.0219
a_{22}	0.0235	0.0254	0.0277	0.0237	0.0259
a_{12}	0.0009	0.0004	0.0010	0.0038	0.0008
a_{21}	0.0052	0.0070	0.0097	0.0050	0.0055
E_x	0.0152	0.0029	-0.0028	0.0466	0.0086
E_y	-0.0119	0.0038	0.0241	-0.0012	-0.0252
R^2 D_x	74.3%	82.8%	88.8%	82.4%	77.8%
R^2 D_y	75.2%	83.4%	84.2%	88.4%	77.0%

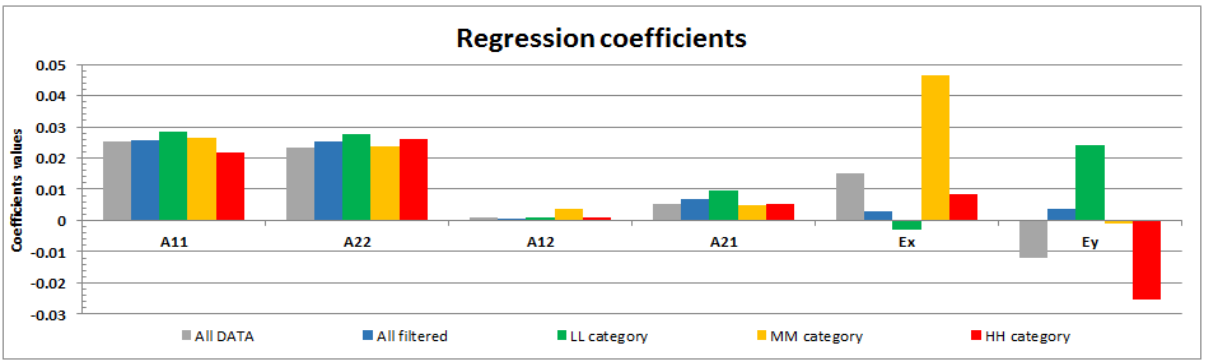

Figure 12. Regression coefficients comparison for various sets of data.

The set of computed coefficients above was subsequently used to hindcast drift for cases with known wind and drift conditions based on GFS forecast data archive. As an example, a single ice floe has been tracked for period of almost 2 weeks (30-Jan-2016 to 12-Feb-2016). The black arrows in Figure 13 (Left) indicate observed ice displacements over the imagery interval periods; green arrows are modeled ice displacement over the same periods using averaged wind

and blue arrows are modeled ice displacement over 3-hours wind interval.

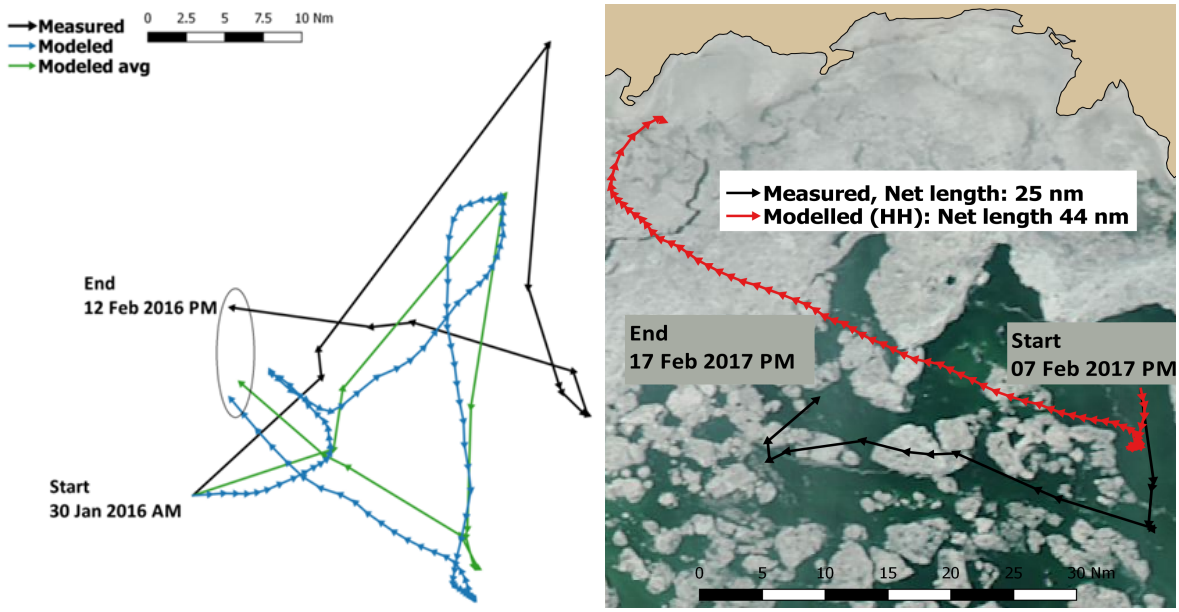

Figure 13. Comparison of measured and modeled ice drift for the periods 30/Jan/2016 to 12/Feb/2016 (Left) and 07/Feb/2016 – 17/Feb/2016 (Right)

Figure 14 shows two samples of modelled drift using GFS data and three different coefficients corresponding to different concentration ratings. These cases show better fit when corresponding set of coefficients is used in different by concentration conditions.

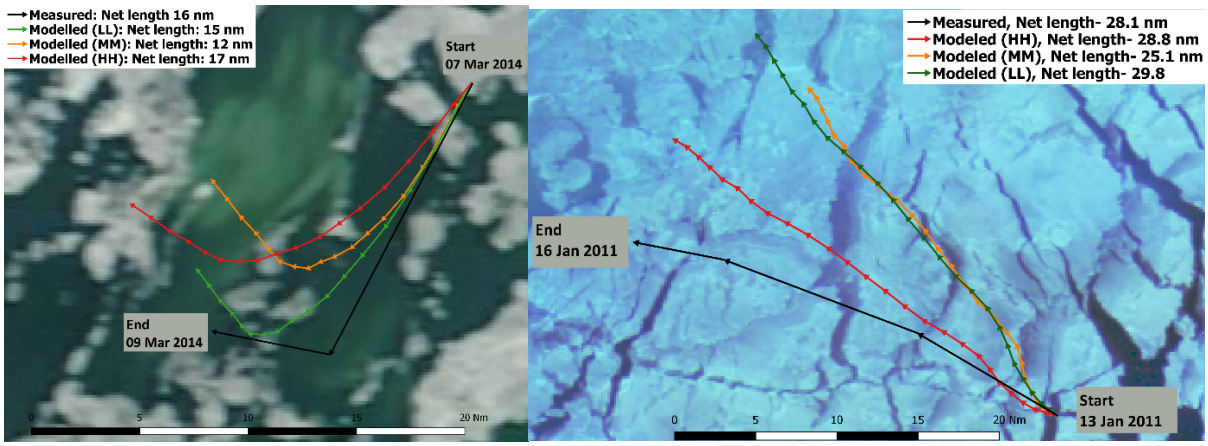

Figure 14. Results of verification in unconfined conditions of low (left) and high (right) concentration.

However, once there is an obstacle or confinement at coastline the model does not show any good fit at all as demonstrated on Figure 13 (Right), when the actual drift has finished in front of stable ice zone along the coastline and the model continued its progress.

DISCUSSION

The values of a_{11} and a_{22} for all set of data are between 0.02 and 0.03. The residual drift variation (E_x and E_y) values were significant for low wind speeds (especially for MM and HH concentration categories), but become negligible with increasing wind speeds as wind starts to dominate over other factors.

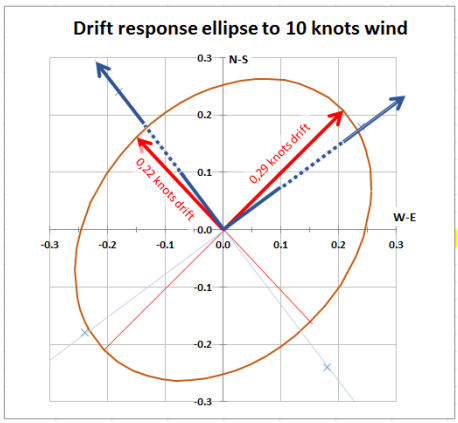

Figure 15. Drift response ellipse to wind speed circle of 10 knots.

The coefficients a_{12} and a_{21} are mostly much smaller than a_{11} and a_{22}, except for several cases when a_{21} almost reaches 0.01 for LL category, meaning that for Low concentrations wind zonal component (W-E) tends to influence drift meridional component (N-S) turning the drift vector a bit to the left from wind vector. Apparently positive a_{12} and a_{21} coefficients show that the response of ice depends not only on wind speed, but also on wind direction. To demonstrate this effect, the ice drift response ellipse was built (**Error! Reference source not found.**).

It shows the response of the ice to circumferential wind with constant speed of 10 knots. For wind of 10 knots in NE and NW direction (blue vectors) ice will tend to drift in the same direction with slight deviation to the left (red vectors). The general idea is that drift speed in NE or SW directions (big semi-axis), for example, tends to be almost 30% higher than for NW or SE (small semi-axis) for the same wind speed. These results make sense for the NE Caspian Sea (Figure 1), that has NE-SW stretched form and fast ice forming along coastlines creates confinement for mobile ice to easily drift in NE and SW directions.

CONCLUSIONS

The major achievement of this project is that a reliable dataset of ice drift in the region was compiled for the season 2015-2016. The dataset was used to gain initial understanding of how ice responds to wind in the conditions of the Caspian basin. Ice moves with 2 to 3% of wind speed for 41% of tracks and between 1-4% for about 90% of tracks. Correlation of wind direction to resulting drift direction was challenging due to many factors guiding the process. The method chosen to correlate wind and drift vectors could be used as a working solution for variable concentrations if there is no confinement of drift with coastline or landfast ice and obstacles in form of stationary ice features or artificial structures.

Introduction of Sentinel constellation with sufficient frequency of reattendance in the region starting last winter (2016-2017) the authors have received opportunity to grow the drift

database and further improve the model. Introduction of additional set of coefficients and logic considering proximity to obstacles and coastline is the most obvious first step for improvement. This work is based on public domain data such as the MODIS Terra and Aqua satellite data and the GFS winds. With higher spatial resolution weather data (for example ECMWF) as well as more SAR satellite imagery to increase frequency of observations could improve the results. Coefficients can also be improved a lot if calibrated with field measurements (e.g. from drift buys) if they were publicly available.

ACKNOWLEDGEMENTS

Sean McDermott has inspired the whole development of the ice project in the history of its development. Authors are grateful to Paul Verlaan for giving his opinion on the work performed and advice on future development of this project. KSAT as the leading provider of SAR imagery in NRT operational mode has been the most significant facilitator of our Ice Charting operations in the Caspian and has contributed in our research with archive SAR images that helps us conduct our research and deliver better analysis to community. Carles Debart has spent significant time on technical discussions with us in regards of using SAR images and support in acquiring archive data.

REFERENCES

Crocker G., Ritch A., Nilsen R., 2011, Some Observations of Ice Features in the North Caspian Sea. *Proceedings of the 21st International Conference on Port and Ocean Engineering under Arctic Conditions,* July 10-14, 2011, Montréal, Canada, POAC11-118.

Jordaan I., Stuckey P., Bruce J., Croasdale K., Verlaan P., 2011, Probabilistic Modelling of the Ice Environment in the Northeast Caspian Sea and Associated Structural Loads. *Proceedings of the 21st International Conference on Port and Ocean Engineering under Arctic Conditions,* July 10-14, 2011, Montréal, Canada, POAC11-133.

Leppäranta, M. 2005. *The Drift of Sea ice*. Praxis Publishing Ltd., Chichester, UK.

Nilsen R., Verlaan P.A.J., 2011, The North Caspian Sea Ice Conditions and how Key Ice Data is Gathered. *Proceedings of the 21st International Conference on Port and Ocean Engineering under Arctic Conditions,* July 10-14, 2011, Montréal, Canada, POAC11-112.

Segboer T.J. and Verlaan P.A.J., 2007, Ice Drift Under the Influence of Winds and Currents along the Sakhalin Northeast Coast. 2007 Dalian University of Technology Press, Dalian, ISBN 978-7-5611-3631-7

Verlaan P.A.J., Croasdale K. 2011, Ice Issues Relating to the Kashagan Phase II Development, North Caspian Sea'. *Proceedings of the 21st International Conference on Port and Ocean Engineering under Arctic Conditions,* July 10-14, 2011, Montréal, Canada, POAC11-171.

Yamartino, R. J., 1984. A Comparison of Several "Single-pass" Estimators of the Standard Deviation of Wind Direction. J. Climate Appl. Meteor., Vol. 23, pp.1362-l366

Raw Data Sources: NASA worldview portal, NOAA National Centers for Environmental Information, GFS weather model data, Copernicus Science Hub